Fault Location on Transmission Lines Based on Travelling Waves Using Correlation and MODWT

V. Gonzalez-Sanchez, V. Torres-García, and D. Guillen

***Abstract*—This paper presents a protection scheme for alternating current transmission lines based on the traveling wave propagation. The analyzed protection scheme uses measurements in only one terminal by using the distributed parameter theory. The method analyzes the fault location using the correlation between two traveling waves, backward and forward waves. Results demonstrate that the correlation method can accurately estimate the fault distance, and this is carried out by using the first two wavefronts of the arrived signals at the measurement terminal. The algorithm is validated through the IEEE 9-bus test system, considering different faults simulated in the software ATP-EMTP. The studied method's effectiveness is assessed and compared with the MODWT, showing both techniques good results for the fault location process.**

***Index Terms*—Fault Location, Transmission Lines, Traveling Waves, Correlation, MODWT, Transients.**

I. Introduction

ELECTRIC power systems must guarantee a continuous power supply and must be reliably and safely during the most operating conditions to avoid large blackouts. This fact demands advanced protection systems to interrupt the fault currents, allowing faster disconnection of the damaged equipment. Due to the generated energy travels from long distances using overhead transmission lines, which are exposed to different transient phenomena such as lightning, short circuits, overloads, and aging. Therefore, if a fault occurs on any transmission line, its location must be estimated to carry out the restoration actions to recover its normal operation [1]. The restoration time may be accelerated if the fault location is accurately estimated. On the contrary, faults can propagate to other power equipment, resulting in high economic losses for the utilities and customers [2].

Among the fault location methods, the most used are those based on impedance because they are economical and easy to implement [3]. These algorithms use the estimated apparent impedance, but they may be affected by high-frequency transients. Currently, with the development of modern computer processors, new algorithms have been implemented to reduce the clearing time of faults by considering high-frequency components into their operation. The accuracy and speed obtained with the traveling wave-based methods are higher than those based-impedance methods. In addition, traveling wave-based methods can be practically used in any transmission line, including transmission lines with series compensation, parallel transmission lines, and even on DC transmission lines with quite similar precision and speed; therefore, the utilization is justified [4].

Traveling waves are high-frequency electromagnetic pulses propagating in both directions on a transmission line from the fault point. Each transmission line has a different propagation speed according to its physical characteristics. If there is a fault, the wavefronts are defined by the signal's arrival time at each transmission line terminal [5]. Therefore, the fault location is carried out by considering the total line length and the wavefronts. To this purpose, transient signals are processed to determine when a fault occurs.

Several algorithms have been developed to process transient signals. Some techniques use the first wavefront arrival time that reaches each terminal. Other techniques use the frequency components at only one end of the line, which is based on the fact that each end of the line presents a large discontinuity to generate traveling waves that reach both ends of the line [6]; those waves will be reflected and refracted in the faulted line.

A large number of techniques have been studied to identify traveling waves. For example, the wavelet transform (WT) has been widely used to analyze traveling waves in transmission lines. In [7], a combination of single-ended and double-ended techniques to determine the fault location is presented.

A fault location method for single-phase-to-ground faults based on the traveling wave's time-frequency characteristics is proposed in [8]. This method analyzes the first arrival time of the traveling wave by using wavelet analysis, and the matrix pencil algorithm is applied to obtain the velocity of the incident wave. The fault distance is calculated using the difference of the wave's speed. In [9], a comparison between different fault location algorithms is presented, a wavelet-based fault location algorithm is introduced, which claims to be more accurate than time-domain and impedance methods.

Some techniques also use functions to correlate two sections of a signal to identify the reflected traveling waves from the fault point. In [10], an ultra-high-speed relay based on the correlation of incremental quantities is proposed. A correlation method of the traveling waves generated by faults in distribution lines is proposed in [11]. A correlation between theoretical frequencies and characteristic frequencies inferred from the transient spectrum is carried out. In [12], a fault location algorithm using the time differences of the arrival times of traveling waves is presented, and an objective function is used to estimate the fault distance. A single-ended fault location method is presented in [13]; that proposal determines the fault location using a correlation process where a reference

V. Gonzalez-Sanchez is with Posgrado de Ingeniería, Universidad Nacional Autónoma de México, CDMX, México, e-mail: victorhugogonzalez-sanchez@comunidad.unam.mx.

V. Torres-Garcia is with Departamento de Energía Eléctrica, Universidad Nacional Autónoma de México, CDMX, México, e-mail: v.torres@ieee.org

D. Guillen is with Escuela de Ingeniería y Ciencias, Tecnológico de Monterrey, Nuevo León, México, e-mail: guillenad@tec.mx.

This work was supported in part by UNAM PAPIIT: IA106420.

is compared against transient signals caused by faults.

There are several challenges in implementing algorithms that use traveling waves to locate faults in transmission lines. For example, the time of synchronization in two-terminal methods is studied by other researchers. In [14], a traveling wave method to locate faults in a multi-terminal transmission line is presented, where a measurement device senses the current at the midpoint of each branch, which uses time synchronization for the measurements. A two-terminal traveling wave method to locate faults in a transmission line is proposed in [15]; this algorithm does not require data synchronization. An improved single-end traveling wave method for fault location on transmission lines connected to short lines is presented in [16]. The algorithm requires three fault recorders to be installed on the line. Besides, [17] summarizes some issues associated with traveling wave-based methods of one terminal.

In this paper, a traveling wave-based fault location method using the correlation technique is presented to locate faults in alternating current (AC) transmission lines; this proposal uses measurements at one terminal of the line, avoiding the persistent problem of synchronization. The fault distance estimation is carried out using a correlation method, and this is compared with the modified discrete wavelet transform (MODWT) technique.

The main contribution of the paper is the analysis and implementation of the correlation-based traveling wave method. The performance of the discussed method is also compared similarly with the MODWT method. In addition, its effectiveness is tested against different fault types, fault resistances, signals with noise, and the sampling frequency is also evaluated. The results show that both analyzed methods present good performance, but the main limitation of the correlation-based traveling wave method is that it is susceptible to high noise levels, and its effectiveness is only guaranteed to noise levels greater than 50 decibels (dB).

II. Transmission Line of Distributed Parameters

A transmission lossless line model is utilized by convenience to study traveling wave propagation during faults . For example, Fig. 1 presents a lossless transmission line consisting of two wires of length l. At the sending node, there is a single-phase equivalent with an impedance $Z_S(s)$, and a load impedance $Z_R(s)$ is taken into account at the receiving node. The characteristic impedance Z_C associated with the transmission line parameters must be known to analyze the traveling waves on transmission lines. Based on the last assumptions, and analyzing the circuit shown in Fig. 1, let consider that the switch sw closes; therefore, the traveling wave starts propagating along the line, and its behavior will depend on the connected load, especially when there is a short circuit or an open circuit in the transmission line.

By using Fig. 1 and bearing in mind Kirchhoff's laws, the equations that describe the voltage profiles along the lossless transmission line (per length unit x), and the currents per each section of the distributed parameters are [18]–[20]:

$$u_x(x,t) = -Li_t(x,t) \tag{1}$$

$$i_x(x,t) = -Cu_t(x,t) \tag{2}$$

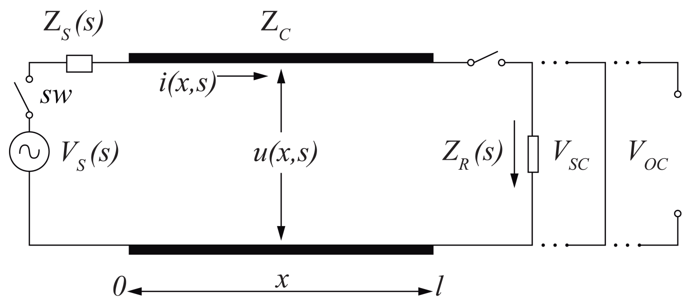

Fig. 1. Transmission line model of distributed parameters with no losses using the Laplace domain.

where $u_x(x,t)$ and $i_x(x,t)$ are the partial derivatives with respect to x for voltages and currents, respectively. $u_t(x,t)$ and $i_t(x,t)$ represent the partial derivatives of voltage and current with respect to t, respectively. L and C define the transmission line's characteristic impedance, and both represent its inductance and capacitance.

Equations (1) and (2) can be expressed in terms of the propagation speed v of the voltage wave traveling along the transmission line. Therefore, the reduced expression for the traveling wave of voltage is,

$$u_{tt}(x,t) - v^2 u_{xx}(x,t) = 0 \tag{3}$$

The solution for (3) can be determined assuming the initial conditions, equal to zero, and this leads to finding the general solution in Laplace domain [18]:

$$u(x,s) = V^-(s)\,e^{-\frac{sx}{v}} + V^+(s)\,e^{\frac{sx}{v}} \tag{4}$$

where V^- represents the voltage traveling wave in the forward direction and V^+ the voltage traveling wave in the backward direction.

On the other hand, when the initial conditions are different from zero, the general solution of (3) can be defined as follows [21]:

$$\begin{aligned} u(x,s) &= V^+(s)\,e^{-\frac{s}{v}x} + V^-(s)\,e^{\frac{s}{v}x} \\ &\quad - \frac{1}{sv}\int_0^x [su(y,0)+u_t(y,0)]\left(\frac{e^{\frac{s}{v}x} - e^{-\frac{s}{v}x}}{2}\right)dy \end{aligned} \tag{5}$$

Considering the following boundary conditions of the transmission line at points $x=0$ and $x=l$, the equations are:

$$\begin{aligned} u(0,s) &= V_S(s) - Z_S(s)i(0,s) \\ u(l,s) &= Z_R(s)i(l,s) \end{aligned} \tag{6}$$

Therefore, the solution for voltage along the transmission line, per unit length x, is obtained as follows [21]:

$$\begin{aligned} u(x,s) = &\frac{V_S(s)\,(1-\Gamma_S(s))}{2\left(1-\Gamma_S(s)\,\Gamma_R(s)\,e^{\frac{2sl}{v}}\right)}\times \\ &\left(e^{-\frac{sx}{v}} + \Gamma_R(s)\,e^{-\frac{2sl}{v}}e^{\frac{sx}{v}}\right) \end{aligned} \tag{7}$$

where $\Gamma_S(s)$ and $\Gamma_R(s)$ define the reflection coefficients at the sending and receiving nodes, respectively [18]–[20]. These reflection coefficients are defined by the line's characteristic impedance, $Z_C = (L/C)^{1/2}$.

$$\Gamma_S(s) = \frac{Z_S(s) - Z_C}{Z_S(s) + Z_C} \tag{8}$$

$$\Gamma_R(s) = \frac{Z_R(s) - Z_C}{Z_R(s) + Z_C} \tag{9}$$

The mathematical description of traveling waves presented above allows understanding waves' propagation during fault events in transmission lines. Therefore, the fault location is a process performed in protection relays by using digital implementations. This entails a numerical analysis in the discrete domain, which is discussed in the following section.

III. Traveling wave using single-end signals

Faults on transmission lines generate changes in the voltage and current signals coming from a steady-state, where the new voltages and currents can be computed as:

$$u(t) = u(t) + \Delta u(t) \tag{10}$$

$$i(t) = i(t) + \Delta i(t) \tag{11}$$

Bearing in mind the relationship between the voltage u and the current i for a distributed parameter model, the time domain solution with respect to the line length x is fully described by the telegrapher's equation [22]. In fact, the numerical solution of the telegrapher's equation can be expressed in terms of traveling waves, backward f_1 and forward f_2, such as:

$$u(x,t) = f_1(x - vt) + f_2(x + vt) \tag{12}$$

$$i(x,t) = \frac{1}{Z_c}\left[f_1(x - vt) - f_2(x + vt)\right] \tag{13}$$

where v is the speed propagation.

The backward and forward traveling waves can be expressed in terms of incremental quantities of voltage Δu and current Δi, such as:

$$S_1(t) = 2f_1(t) = \Delta u(t) + Z_c\Delta i(t) \tag{14}$$

$$S_2(t) = 2f_2(t) = \Delta u(t) - Z_c\Delta i(t) \tag{15}$$

where S_1 is the backward wave, and S_2 is the forward wave. These signals S_1 and S_2 are employed by distance relays based on traveling waves to estimate the fault distance when a fault occurs.

A. Modal transformation

The coupling phenomenon between phases due to mutual inductances may be neglected to analyze traveling waves' propagation in transmission lines. This means that the voltages and currents have to be processed by employing modal transformations because these simplify the numerical calculus, quite similar to a single-phase system. The most common transformation matrices are defined by Clarke's transform, Wedepohl's transform, and Karrenbauer's transform. Each transformation matrix allows obtaining three propagation modes, two aerial modes, and one zero mode. The aerial modes are not affected by the frequency, and their propagation speed is very close to the light speed. The zero mode represents the zero sequence component, where both the propagation speed and the attenuation of traveling waves are affected by the ground resistivity as well as by the fault type. In this paper, aerial modes 1 and 2 are used to estimate the fault distance when a fault occurs along the transmission line. Besides, this work uses Clark's transform to calculate the modal components [23]:

$$\begin{bmatrix}\Delta u^{(0)} \\ \Delta u^{(1)} \\ \Delta u^{(2)}\end{bmatrix} = \frac{1}{3}\begin{bmatrix}1 & 1 & 1 \\ 2 & -1 & -1 \\ 0 & \frac{1}{\sqrt{3}} & -\frac{1}{\sqrt{3}}\end{bmatrix} = \begin{bmatrix}\Delta u_a \\ \Delta u_b \\ \Delta u_c\end{bmatrix} \tag{16}$$

By using a modal transformation and substituting in expressions (14) and (15), the forward and backward traveling waves can be computed in the modal domain by:

$$\begin{aligned} S_1^{(m)} &= \Delta u^{(m)} + Z_c^{(m)}\Delta i^{(m)} \\ S_2^{(m)} &= \Delta u^{(m)} - Z_c^{(m)}\Delta i^{(m)} \end{aligned} \tag{17}$$

where $S_1(m)$ and $S_2(m)$ are known as traveling wave signals, and the superscript m represents the propagation mode used.

Each propagation mode has different speeds and different impedances. For instance, the zero mode is used to locate phase-to-ground faults, whereas the second propagation mode can be used to locate non-phase-to-ground faults. The first aerial mode can be used to locate any fault type [24]. For this reason, in this research, a conditional statement is used in the algorithm to decide between the most appropriate aerial mode to detect the fault, the zero mode is avoided for the reasons mentioned above.

B. Fault detection and directional discrimination

Although the signals S_1 and S_2 can be used to estimate the fault distance, both signals should be processed to improve the fault identification, especially to include the directionality in distance relays as reported in [23]. This is carried out by two discrimination functions shown below:

$$d_f = \sqrt{\left(S_1^{(m)}\right)^2 + \left[\frac{1}{\omega}\frac{d}{dt}\left(S_1^{(m)}\right)\right]^2} \tag{18}$$

$$d_r = \sqrt{\left(S_2^{(m)}\right)^2 + \left[\frac{1}{\omega}\frac{d}{dt}\left(S_2^{(m)}\right)\right]^2} \tag{19}$$

If both the signals d_f and d_r exceed a predetermined setting value, a fault condition will be detected. The fault's directionality will be determined by following the sequence of the signals d_f and d_r, that is, which one exceeds, firstly, the setting value.

C. Correlation function

The cross-correlation between two signals defines the similarity between them. Therefore, the distance estimation during faults on transmission lines can be carried out using the correlation, as was proposed in [25].

The correlation function is described as follows:

$$\Phi_{S_1S_2}(m\Delta t) = \frac{1}{N}\sum_{k=1}^{N}\left[S_2(k\Delta t) - \overline{S_2}\right]\left[S_1(k\Delta t + m\Delta t) - \overline{S_1}\right] \tag{20}$$

where:

$$\overline{S_1} = \frac{1}{N}\sum_{k=1}^{N} S_1(k\Delta t + m\Delta t) \tag{21}$$

$$\overline{S_2} = \frac{1}{N}\sum_{k=1}^{N} S_2(k\Delta t) \tag{22}$$

where $\overline{S_1}$ and $\overline{S_2}$ represent the average of their respective sample groups. The correlation function indicates the closest similarity between both waveforms; therefore, the passed away time where the maximum correlation occurs can be used to determine the distance to the fault point.

D. Modified discrete wavelet transform

The signals $S_1(m)$ and $S_2(m)$ can also be processed by using the Modified Discrete Wavelet Transform (MODWT), this implies that the incremental quantities of voltage Δu and current Δi may generate new coefficients defined by [26]:

$$\Delta u_w^{(m)}(p) = \sum_{l=1}^{N} h(l)\Delta u(p + l + N) \tag{23}$$

$$\Delta i_w^{(m)}(p) = \sum_{l=1}^{N} h(l)\Delta i(p + l + N) \tag{24}$$

where p is the actual sample, N is the number of samples of a data window and $h(l)$ is the wavelet filter defined by the mother wavelet.

The new signals that will be used to the fault location are defined as follows:

$$\begin{aligned} S_{1w}^{(m)} &= \Delta v_w^{(m)} + Z_c^{(m)}\Delta i_w^{(m)} \\ S_{2w}^{(m)} &= \Delta v_w^{(m)} - Z_c^{(m)}\Delta i_w^{(m)} \end{aligned} \tag{25}$$

E. Estimation of fault location

Once the first incident wave and the reflected wave from the fault point have been identified and considering the propagation speed of the traveling waves, the fault distance can be estimated as follows [23]:

$$d = \frac{(t_2 - t_1)v}{2} \tag{26}$$

where t_1 and t_2 correspond to the first wavefront arrival time and its subsequent reflection coming from the fault point, respectively. In this case, v is the propagation speed of the traveling waves in the transmission line.

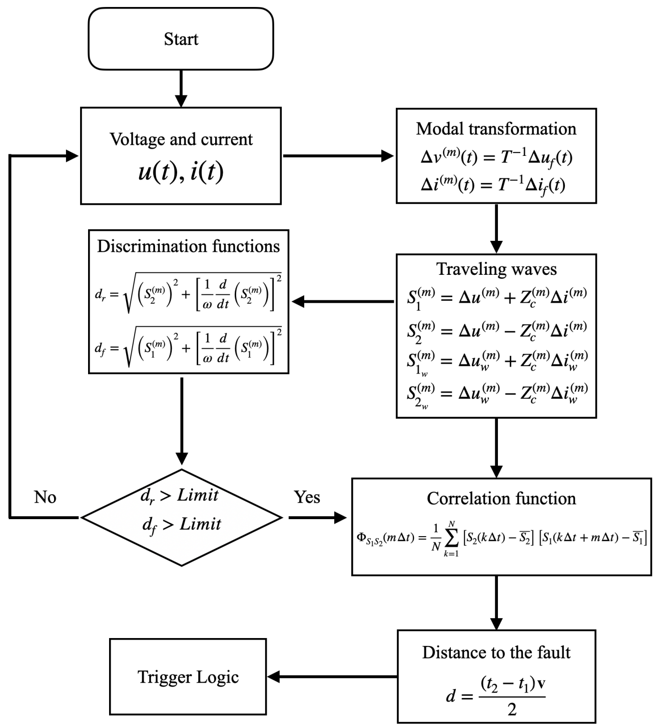

Fig. 2. Flow chart showing the algorithm for determining the distance to a fault on a transmission line

The algorithm utilized for locating faults on transmission lines is summarized in Fig. 2. First, the discrete signals of voltage and current are analyzed through a modal transformation matrix represented by T. Next, the traveling wave signals must be obtained, which are used to determine if there is a fault condition. Then, the signals d_f and d_r are analyzed to identify fault conditions, and this entails that a fault can be detected when both signals exceed a setting value. Last, the correlation function is computed to find the passed away time between the first incident wave and its reflection on the measurement terminal. Finally, once the arrival times are known, the fault point is estimated.

IV. Case of Study

The well-known IEEE 9-bus test system is used to test the effectiveness of the algorithm described above. This power system consists of three synchronous machines, nine buses, six transmission lines, three step-up transformers, and three loads. The total load demand is 315 MW and 115 MVAr [27]. For this test system, the longest transmission line corresponds to line 6-9, connecting buses 6 and 9. This line is chosen for testing the fault location algorithm, where the line length is 179.86 km.

In this paper, the measurement terminal is located on bus 6. Besides, a J Marti [28] distributed parameter model is used due to its characteristics for a wide range of frequencies as well as its numerical stability; this model also offers a good response to analyze traveling waves methods [29]. Therefore,

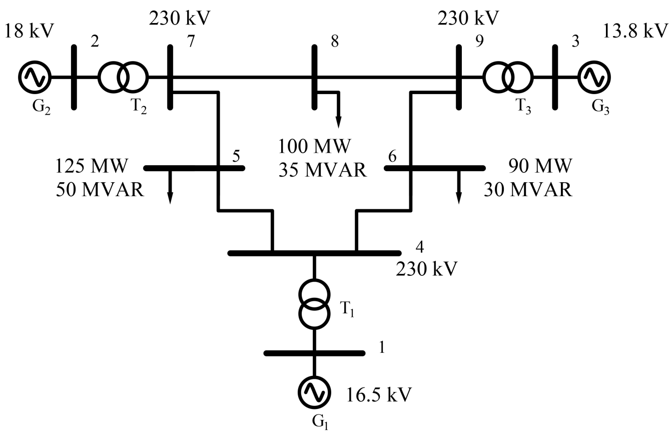

Fig. 3. IEEE 9-bus test system used to validate the fault location algorithm.

the correlation-based traveling wave method is proved considering a characteristic impedance of $Z_C = 365.057\Omega$. In addition, the propagation speed of aerial modes 1 and 2 is $v = 274478.8648 \frac{m}{s}$.

V. Results and Simulations

The fault analysis is carried out by using the system shown in Fig. 3. Three-phase, two-phase, and single-phase to ground faults were simulated using intervals of 20 km along the transmission line. Besides, many fault resistances were considered in the simulations with a maximum value of 100 Ω. The effect of noise is also analyzed.

For example, a three-phase to ground fault was simulated at 20 km of the transmission line; the voltages and currents in the abc reference frame are shown in Fig. 4. For this case, the fault was simulated at $t = 0.02s$.

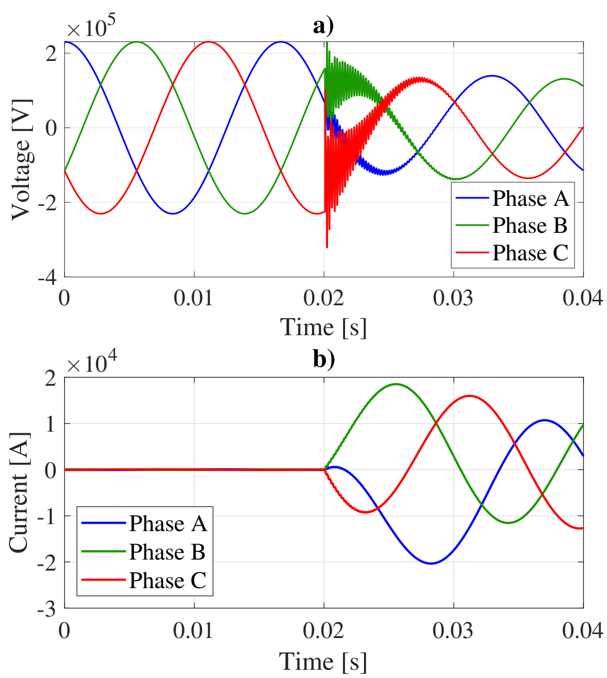

Fig. 4. Voltage and current signals for a three-phase fault at 20 km on the transmission line.

The modal transformation is used to decouple the electrical signals of the three-phase system into three propagation modes. The aerial mode 1 is used to find the traveling wave signals S_1 and S_2; these signals are shown in Fig. 5(a). Also, the resulting signal of correlation between S_1 and S_2 is shown in Fig. 5(b), where the maximum value of the signal indicates the greatest similarity between both signals. In a similar way, the signals S_{1w} and S_{2w} are displayed on Fig. 6.

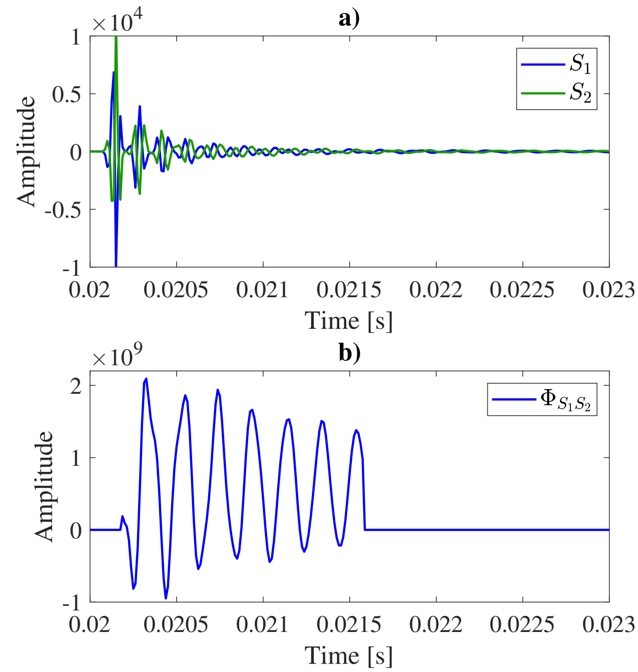

Fig. 5. Signal processing to identify the arrival times of incident waves. (a). Traveling wave signals S_1 and S_2 for three-phase fault at 20 km. (b). Correlation signal of S_1 and S_2 for three-phase fault at 20 km.

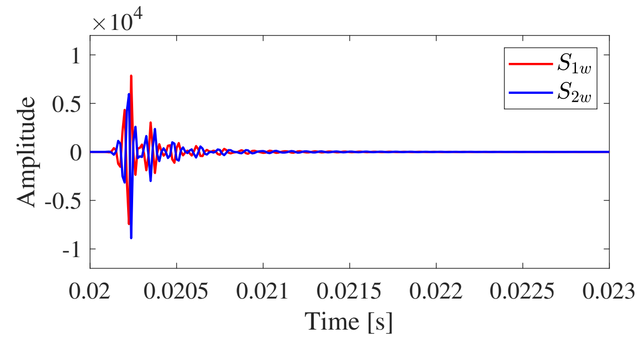

Fig. 6. Traveling wave signals S_{1w} and S_{2w} for three-phase fault at 20 km.

The propagation speed of the traveling waves regarding the fault location on different points of the transmission line is shown in Fig. 7. Based on the results, the first wavefront is displaced according to the MODWT, depending on the fault location. Notice that similar behavior occurs for the second wavefront with respect to the first wavefront.

As previously mentioned, the discrimination functions help identify the fault condition, when exceeding a pre-established threshold; quite similar to another work based on threshold for fault detection [29].

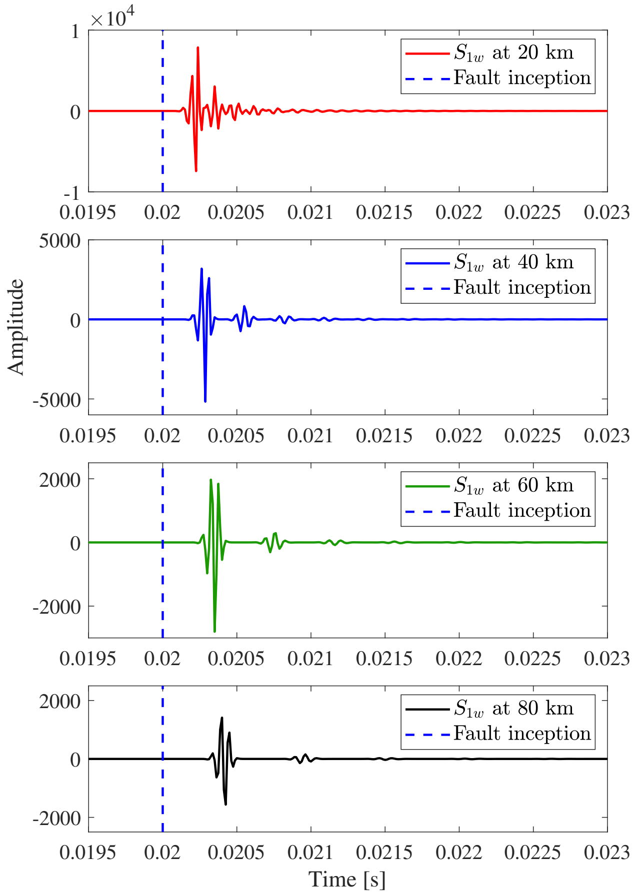

Fig. 7. Wave propagation for different fault locations by using MODWT.

To generalize the proposed method, the threshold is determined by analyzing the signals d_f and d_r. According to (18) and (19), when there is no fault condition along the transmission line, this means that the signals S_1 and S_2 will not present any change, therefore, their derivatives tend to be zero, and the remaining signals are:

$$d_f = \sqrt{\left(S_1^{(m)}\right)^2} \tag{27}$$

$$d_r = \sqrt{\left(S_2^{(m)}\right)^2} \tag{28}$$

The threshold value can be computed using the root mean square of the maximum values of the signals S_1 and S_2 as indicated in the following equation:

$$th = k\sqrt{\frac{\max\left(S_1^{(m)}\right)^2 + \max\left(S_2^{(m)}\right)^2}{2}} \tag{29}$$

where k represents a sensitivity factor because this allows greater sensitivity when there are noisy signals and it is an analogy to the adaptive threshold values of line protections [33,34]. For example, if it is required to have greater robustness against noise, factor k will be adjusted and it recommends values $1 < k \leq 5$. In this work, for the system of Fig. 3, $k = 5$ and $th = 2 \times 10^7$.

Besides, if d_r exceeds the threshold faster than d_f, the fault is downstream on the measurement position. These signals can be seen in Fig. 8, where it can notice that both d_r and d_f exceed the threshold at $t = 0.0201s$. This indicates that the first traveling wave caused by the fault reaches the measurement terminal at that time because the fault is downstream of the relay.

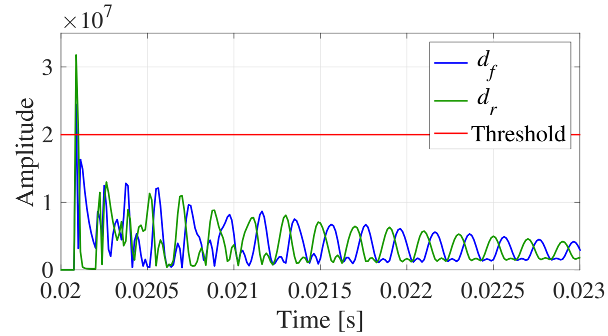

Fig. 8. Setting value and directional signals for a three-phase fault at 20 km.

The correlation function is used to find the passed away time when the first traveling wave is reflected from the fault point. A portion of the signal S_2 is correlated with subsequent portions of the signal S_1. Therefore, the time that produces the maximum correlation will occur when both signals are in phase, and this will be used to find the distance to the fault point according to equation (26). Table I shows the obtained results of the algorithm based on correlation, including the most common types of faults and taking into account several distances.

TABLE I
FAULT LOCATION FOR THE LINE 6-9 BY USING THE CORRELATION ALGORITHM.

Distance	Fault type						
	ABCG	ABG	BCG	ACG	AG	BG	CG
20 km	19.797	19.797	19.797	19.797	19.797	19.797	19.797
40 km	39.594	41.394	39.594	39.594	39.594	39.594	39.594
60 km	59.391	61.191	59.391	59.391	61.191	61.191	61.191
80 km	79.188	80.988	79.188	79.188	80.988	80.988	80.988
100 km	98.985	98.985	98.985	98.985	98.985	98.985	98.985
120 km	116.98	118.78	116.98	116.98	118.78	118.78	116.98
140 km	138.58	140.38	138.58	134.98	140.38	140.38	140.38
160 km	158.38	156.58	158.38	158.38	158.38	156.58	156.58

An exhaustive analysis of the effect of the sampling frequency allows to define operating margins and ensure the reliability of the protection scheme [30]. As discussed in other investigations, the traveling waves-based methods require high sampling rates to have good resolution and accuracy [31]. However, it has been shown that with an average sample rate of some tens of kHz, fast operating time and reasonable accuracy are obtained; furthermore, no special measuring instruments or powerful processors are required [5]. In this work, the algorithm shows good effectiveness using sampling frequencies upper to 80 kHz. The faults simulated in ATP/EMTP with this sampling frequency show an excellent precision to find the arrival times in traveling waves-based methods [32].

The correlation method is also assessed in a noisy environment; this entails adding noise to the voltage and current signals. For example, the results for a three-phase fault at 20 km from the measurement terminal are shown in Fig. 9. For this case, it is considered 50 dB into the voltage and current signals. It is observed that the processed signals are highly affected by the introduced noise. However, the correlation method can be adjusted (algorithm's threshold) to ensure good performance for noisy signals. The results show that the correlation method generates good results for the analyzed case because the estimated distance is 19.797 km, being this an acceptable result. However, the results may not be guaranteed for a lower noise level than 50 dB as this implies greater distortion in the signals.

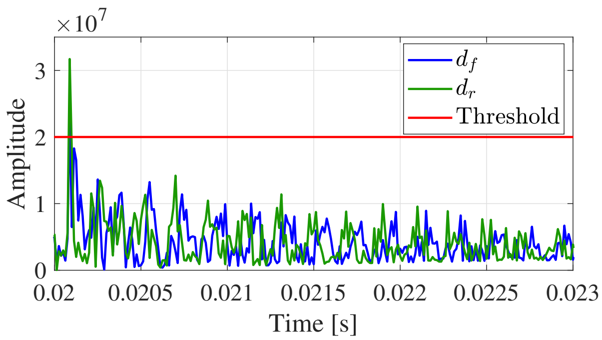

Fig. 9. Setting value and directional signals for a three-phase fault at 20 km with 50 dB of added noise.

Additionally, various cases with different fault resistances were simulated to evaluate the correlation technique for several fault conditions. It was found that the method shows promising results with R_f up to 100 Ω. Nevertheless, for phase-to-ground faults, after 160 km from the measurement terminal, with R_f greater than 100 Ω, the method may not be able to detect the reflected traveling waves from the fault point, producing an error in the distance estimation. Table II shows the results obtained for faults with a R_f of 100 Ω.

TABLE II
FAULT LOCATION FOR THE LINE 6-9 BY USING THE CORRELATION ALGORITHM - $R_f = 100\,\Omega$

Distance	Fault type						
	ABCG	ABG	BCG	ACG	AG	BG	CG
20 km	19.80	19.80	19.80	19.80	19.80	19.80	19.80
40 km	39.59	39.59	39.59	39.59	39.59	39.59	39.59
60 km	59.39	61.19	59.39	59.39	61.19	61.19	61.19
80 km	79.19	80.99	79.19	79.19	80.99	80.99	80.99
100 km	98.98	100.78	98.98	98.98	98.98	98.98	98.98
120 km	116.98	118.78	116.98	116.98	118.78	118.78	118.78
140 km	138.58	138.58	138.58	136.78	140.38	138.58	140.38
160 km	158.38	160.18	158.38	158.38	0.00	35.99	35.99

Finally, Table III shows the comparison results (for three-phase faults) between the correlation algorithm and the algorithm based on the MODWT. The results demonstrate a good performance of the analyzed algorithms, and both results are quite similar. Therefore, the distance protection based on one-end traveling wave methods is an efficient method to carry out the fault location on transmission lines.

TABLE III
COMPARISON RESULT USING THE MODWT AND THE CORRELATION ALGORITHM.

Distance	MODWT		Correlation	
	Estimated	Error (%)	Estimated	Error (%)
20	19.7970	0.1128	19.797	0.1128
40	39.5940	0.2256	39.594	0.2256
60	59.3909	0.3384	59.391	0.3383
80	79.1879	0.4512	79.188	0.4511
100	98.9849	0.5640	98.985	0.5639
120	118.7819	0.6767	116.98	1.6778
140	140.3786	0.2103	138.58	0.7889
160	158.3758	0.9023	158.38	0.9000

VI. CONCLUSION

In this paper, an implementation of an algorithm to locate faults accurately in a transmission line is presented. The method is based on one terminal that requires voltage and current measurements, which represents an advantage since time synchronization errors are avoided, in addition to the fact that a communications channel is not required. The correlation method and the MODWT based method were used to obtain the traveling wave signals, which are processed to determine the forward wave propagation and reflected waves generated by faults.

Both algorithms were tested using the IEEE 9-bus test system, and it was implemented in *ATP/EMTP*™. The algorithms were processed in MATLAB® to assess several fault conditions on the transmission line that connects buses 6 and 9. The results show that the evaluated algorithms produce small errors, around 1.6% using correlation and less than 1% by using MODWT. In this sense, this work demonstrates the effectiveness of both techniques during fault location in transmission lines. It should be mentioned that both techniques have disadvantages in their implementation. Although the correlation method has shown promising results, the method loses precision when the sampling frequency is lower than 80 kHz.

Likewise, a study was carried out to know the influence of noise on the input signals. It was found that noise levels lower than 50 dB, the correlation method loses accuracy; on the contrary, the MODWT technique may include an additional stage for conditioning the input signals. As a consequence of that, this is not so sensitive to noise as the correlation is. Although both techniques offer fast operation, the correlation uses fewer computation operations, in such a sense, the correlation method is faster than the MODWT based method.

The choice of the most suitable technique for locating faults in transmission lines will depend on many factors such as ease of implementation, robustness, flexibility, and adaptability to real applications. Based on the obtained results, it is possible to design an improved scheme that integrates both reviewed techniques to offer better results and a faster estimation for fault location.

REFERENCES

[1] J. Ma, Y. Shi, W. Ma, and Z. Wang. Location method for interline and grounded faults of double-circuit transmission lines based on distributed parameters. *IEEE Transactions on Power Delivery*, 30(3):1307–1316, 2015.

[2] J. Liang, T. Jing, H. Niu, and J. Wang. Two-terminal fault location method of distribution network based on adaptive convolution neural network. *IEEE Access*, 8:54035–54043, 2020.

[3] T. P. S. Bains, T. S. Sidhu, Z. Xu, I. Voloh, and M. R. D. Zadeh. Impedance-based fault location algorithm for ground faults in series-capacitor-compensated transmission lines. *IEEE Transactions on Power Delivery*, 33(1):189–199, 2018.

[4] C. Zhang, G. Song, T. Wang, and L. Yang. Single-ended traveling wave fault location method in dc transmission line based on wave front information. *IEEE Transactions on Power Delivery*, 34(5):2028–2038, 2019.

[5] F. B. Costa, A. Monti, F. V. Lopes, K. M. Silva, P. Jamborsalamati, and A. Sadu. Two-terminal traveling-wave-based transmission-line protection. *IEEE Transactions on Power Delivery*, 32(3):1382–1393, 2017.

[6] O. Naidu and A. K. Pradhan. A traveling wave-based fault location method using unsynchronized current measurements. *IEEE Transactions on Power Delivery*, 34(2):505–513, 2019.

[7] H. A. Abd el-Ghany, A. M. Azmy, and A. M. Abeid. A general travelling-wave-based scheme for locating simultaneous faults in transmission lines. *IEEE Transactions on Power Delivery*, 35(1):130–139, 2020.

[8] Zhao Jianwen, Hou Hui, Gao Yu, Huang Yongping, Gao Shuping, and Lou Jianan. Single-phase ground fault location method for distribution network based on traveling wave time-frequency characteristics. *Electric Power Systems Research*, 186:106401, 2020.

[9] Mahmood Parsi, Peter Crossley, Pier Luigi Dragotti, and David Cole. Wavelet based fault location on power transmission lines using real-world travelling wave data. *Electric Power Systems Research*, 186:106261, 2020.

[10] A. Lei, X. Dong, and V. Terzija. An ultra-high-speed directional relay based on correlation of incremental quantities. *IEEE Transactions on Power Delivery*, 33(6):2726–2735, 2018.

[11] A. K. Apolo Penaloza and G. Dorneles Ferreira. Faulted branch location in distribution networks based on the analysis of high- frequency transients. *IEEE Latin America Transactions*, 16(8):2207–2212, 2018.

[12] R. Liang, N. Peng, L. Zhou, X. Meng, Y. Hu, Y. Shen, and X. Xue. Fault location method in power network by applying accurate information of arrival time differences of modal traveling waves. *IEEE Transactions on Industrial Informatics*, 16(5):3124–3132, 2020.

[13] A. Kulikov, A. Loskutov, and P. Pelevin. Methods for implementing of the single-ended traveling wave fault locating on the transmission lines based on traveling wave pattern recognition. In *2018 International Multi-Conference on Industrial Engineering and Modern Technologies (FarEastCon)*, pages 1–6, 2018.

[14] J. Ding, X. Wang, Y. Zheng, and L. Li. Distributed traveling-wave-based fault-location algorithm embedded in multiterminal transmission lines. *IEEE Transactions on Power Delivery*, 33(6):3045–3054, 2018.

[15] F. V. Lopes, K. M. Dantas, K. M. Silva, and F. B. Costa. Accurate two-terminal transmission line fault location using traveling waves. *IEEE Transactions on Power Delivery*, 33(2):873–880, 2018.

[16] Nan Peng, Lutian Zhou, Rui Liang, and Haoyuan Xu. Fault location of transmission lines connecting with short branches based on polarity and arrival time of asynchronously recorded traveling waves. *Electric Power Systems Research*, 169:184 – 194, 2019.

[17] G. Gemelli, F. Palone, M. Rebolini, and F. Falorni. Factors affecting the single-ended travelling wave-based fault location in hv lines. In *2018 IEEE International Conference on Environment and Electrical Engineering and 2018 IEEE Industrial and Commercial Power Systems Europe (EEEIC / I CPS Europe)*, pages 1–6, 2018.

[18] J.D. Glover, M.S. Sarma, and T. Overbye. *Power System Analysis and Design*. Cengage Learning, 2011.

[19] P. M. Anderson. *Power System Protection*, pages 377–377. New York, McGraw-Hill, IEEE Press, 1999.

[20] A. Greenwood. *Electrical Transients in Power Systems*. Wiley-Interscience, 1971.

[21] V. Torres, J.L. Guardado, H.F. Ruiz, and S. Maximov. Modeling and detection of high impedance faults. *International Journal of Electrical Power and Energy Systems*, 61:163 – 172, 2014.

[22] A. Gopalakrishnan, M. Kezunovic, S. M. McKenna, and D. M. Hamai. Fault location using the distributed parameter transmission line model. *IEEE Transactions on Power Delivery*, 15(4):1169–1174, 2000.

[23] M.M. Saha, J.J. Izykowski, and E. Rosolowski. *Fault Location on Power Networks*. Power Systems. Springer London, 2009.

[24] Zahra Moravej, Masoud Movahhedneya, and Mohammad Pazoki. Gabor transform-based fault location method for multi-terminal transmission lines. *Measurement*, 125:667–679, 2018.

[25] P. A. Crossley and P. G. McLaren. Distance protection based on travelling waves. *IEEE Transactions on Power Apparatus and Systems*, PAS-102(9):2971–2983, 1983.

[26] V. Ashok, Anamika Yadav, and Almoataz Y. Abdelaziz. Modwt-based fault detection and classification scheme for cross-country and evolving faults. *Electric Power Systems Research*, 175:105897, 2019.

[27] P.M. Anderson and A.A. Fouad. *Power System Control and Stability*. IEEE Press power engineering series Power system control and stability. Wiley, 2003.

[28] J. R. Marti. Accurate modelling of frequency-dependent transmission lines in electromagnetic transient simulations. *IEEE Transactions on Power Apparatus and Systems*, PAS-101(1):147–157, 1982.

[29] E. S. Gimarães A. S. Bretas L. U. Iurinic, R. G. Ferraz. Transmission lines fault location based on high-frequency components technique: a general formulation for estimation of the dominant frequency. In *International Conference on Power Systems Transients (IPST2013)*, 2013.

[30] R. L. França, F. Silva jünior, T. Honorato, J. P. Ribeiro, F. Costa, F. Lopes, and K. Strunz. Traveling wave-based transmission line earth fault distance protection. *IEEE Transactions on Power Delivery*, pages 1–1, 2020.

[31] M. Silva, Mário Oleskovicz, and D.V. Coury. A fault locator for three-terminal lines based on wavelet transform applied to synchronized current and voltage signals. volume 4, pages 94–103.

[32] C. Aguilera, E. Orduna, and G. Ratta. Adaptive noncommunication protection based on traveling waves and impedance relay. *IEEE Transactions on Power Delivery*, 21(3):1154–1162, 2006.

[33] E. O. Schweitzer, B. Kasztenny, A. Guzmán, V. Skendzic, and M. V. Mynam. Speed of line protection - can we break free of phasor limitations? In *2015 68th Annual Conference for Protective Relay Engineers*, pages 448–461, 2015.

[34] C. Zhang, G. Song, T. Wang, and X. Dong. An improved non-unit traveling wave protection method with adaptive threshold value and its application in hvdc grids. *IEEE Transactions on Power Delivery*, 35(4):1800–1811, 2020.